Desalination and Water Treatment
www.deswater.com

doi: 10.5004/dwt.2023.29163

282 (2023) 258–264
January

Removal of Methylene Blue by synthesized ECD-GO/Fe_3O_4 composite

Mengqi Zhao[a,b,*], Yuxi Chao[a], Xiaoqing Ma[a], Dejun Chen[a,b], Yinnian Liao[a,*]

[a]*School of Chemical Engineering and Technology, Xinjiang University, Urumqi 830017, PR China, emails: xjzmq@163.com (M. Zhao), egglyn@163.com (Y. Liao), cyx13699984156@163.com (Y. Chao), 1040960805@qq.com (X. Ma), 916466460@qq.com (D. Chen)*
[b]*State Key Laboratory of Chemistry and Utilization of Carbon-Based Energy Resources, Urumqi 830017, PR China*

Received 22 June 2022; Accepted 27 November 2022

ABSTRACT

In this study, sethylenediamine-β-cyclodextrin (ECD)-graphene oxide (GO) supermolecules were synthesized using ECD and GO as starting materials. The magnetic nano-adsorbent (ECD-GO/Fe_3O_4) was prepared by hydrothermal loading Fe_3O_4 nanoparticles. Their structures and magnetic properties were characterized by Fourier transform infrared spectroscopy, thermogravimetric analysis, transmission electron microscopy (TEM) and vibrating sample magnetometer (VSM). The results showed that the mass ratios of ECD, GO and Fe_3O_4 nanoparticles were about 29.1%, 28.4% and 30.2%, respectively. TEM analysis showed that the ECD was spherical when loaded onto the sheet GO surface, and the diameter of ECD-GO/Fe_3O_4 was about 60–70 nm. According to VSM test, ECD-GO/Fe_3O_4 exhibits superparamagnetic properties with a saturation magnetization of 22 emu/g. The adsorbent was used for the removal of methylene blue (MB), and the adsorption process was fitted using adsorption isothermal model and kinetic model. The results show that the Freundlich model and pseudo-first-order model are more suitable to describe the adsorption process of MB on ECDGO/Fe_3O_4. Among them, the adsorption capacity is 53 mg/g, and after four cycles, the removal efficiency of MB is about 69%. The material has certain stability and durability, and the removal process can be successfully applied to the treatment of wastewater containing MB.

Keywords: Magnetic nanoparticles; Graphene oxide; Ethylenediamine-cyclodextrin; Methylene blue; Adsorption

1. Introduction

In the past few decades, with the development of dyes and dyeing industry in China, the problem of dye contamination has been worsening [1,2]. It is worth noting that the pollution caused by methylene blue (MB) and other cationic dyes has become a major environmental problem [3]. MB, which is mainly used as a colorant in cotton, wool and silk, can cause eye and skin diseases and affect the respiratory systems of living organisms [4]. The current methods used to treat dye wastewater include adsorption, flocculation, membrane separation and biological process [4–7]. Among them, adsorption is considered to be one of the most powerful wastewater treatment technologies because it is simple to operate, economical, selective and reproducible [8,9].

Graphene oxide (GO) is water-soluble and has attracted attention for effective water pollution control [10]. As an important derivative of graphene material, the cost of graphene oxide has been within the range of control due to the improvement of the current preparation process. The multiple functional groups (e.g., –O–, –OH, –C=O, –COOH) and high surface area (about 2,630 $m^2\ g^{-1}$) of GO make it a potential adsorbent for MB pollution [11]. It has been reported that GO has more oxygen-rich functional groups and active sites, which can bind to dye molecules through electrostatic attraction and coordination [12,13]. However, if it is used as an adsorbent alone, its effective specific surface area will be reduced due to the π–π bond interaction between adjacent layers in GO during the adsorption process, thus reducing the adsorption capacity [14,15]. At the

* Corresponding authors.

1944-3994/1944-3986 © 2023 Desalination Publications. All rights reserved.

same time, the particle size of GO is very small, and the adsorbed particles are difficult to separate, which will cause health and environmental problems once exposed to the environment [16,17].

β-cyclodextrin is a readily available, safe, clean and biodegradable oligomer. On the one hand, the hydrophobic cavity structure of β-cyclodextrin can accommodate smaller molecules. On the other hand, the rich hydroxyl group in its outer cavity makes it hydrophilic and therefore easily modified by groups [18]. The primary amine of ethylenediamine β-cyclodextrin (ECD) has a good chain structure, which can be connected with carboxylic acids, esters, anhydrides, aldehydes and ketones under mild conditions [19]. It is also an effective intermediate layer for the construction of graphene supramolecular structure. However, the low mechanical strength of ECD limits its application in the adsorption field. Therefore, according to the characteristics of ECD and graphene, the combination of graphene and ECD can overcome these obstacles and help to achieve the superposition of composite properties [17–20]. In addition, the addition of magnetic Fe_3O_4 can better realize the separation and reuse of the composite adsorbent. Li et al. [21] synthesized Fe_3O_4/GON/CA-CDP composite, which showed good adsorption capacity for MB dye under electrostatic attraction, Lewis acid–Lewis base interaction, host-guest supramolecular interaction and π–π interaction.

In this study, ethylenediamine-cyclodextrin (ECD) was stably grafted onto the surface of GO nanoparticles by supramolecular interaction [22] to prepare supramolecular ECD-GO. On the one hand, the high specific surface energy of GO nanoparticles could be reduced, and the defects of uneven particle size distribution and poor biocompatibility caused by agglomeration could be avoided. On the other hand, ECD is a kind of super molecular compound that has a cavity, and can be used as a main body by clathrate "formed by the subject and object, through the ECD by modifying the GO, for the first time the magnetic Fe_3O_4 nanoparticles load to ECD-GO, great use of graphene and its functional properties and magnetic adsorbent of the easy separation and recovery characteristics, ECD-GO/Fe_3O_4 composite adsorbent was prepared for easy separation and recovery. In the research process, in order to effectively improve the adsorption capacity of ECD-GO/Fe_3O_4 for MB, the influence of acidity, adsorption time and initial concentration on the adsorption performance of the adsorbent was explored to achieve the purpose of effectively removing MB from wastewater.

2. Experimental details

2.1. Raw materials and reagents

Ethylenediamine-β-cyclodextrin (ECD), analytical grade, was purchased from Shandong Binzhou Zhiyuan Biotechnology Co., Ltd. Industrial grade graphene oxide (JCGO-95-1-2.6) was procured from Nanjing Yakang Nanotechnology Co., Ltd. Hydrazine hydrate was bought from Shanghai Baika Chemical Technology Co., Ltd, and polyethylene glycol (PEG) and other reagents were procured from Tianjin Zhiyuan Chemical Reagent Co., Ltd.

2.2. Static adsorption experiments of the composite

The adsorption capacity of ECD-GO/Fe_3O_4 composite for MB was evaluated by batch treatment in aqueous solution, and the adsorption process was fitted by Langmuir and Freundlich isotherm models and pseudo-first-order and pseudo-second-order kinetic models. For this purpose, 10 mg of complex was added to 40 mL of MB dye solution (100 mg L^{-1}). Adjust the mixture to reach the right acidity, stir for a while, then strain. The concentration of MB dye at different time intervals was determined by UV-Vis spectroscopy at λ max (664 nm).

The adsorption capacity (q_e, mg g^{-1}) and removal efficiency (E) on the adsorbed MB were calculated by using the following formulae:

$$\text{Adsorption capacity: } q_e = \frac{(C_0 - C_e)V}{m} \tag{1}$$

$$\text{Removal efficiency: } E = \frac{(C_0 - C_e)}{C_0} \times 100\% \tag{2}$$

where C_o and C_e are the initial and equilibrium concentrations of MB (mg L^{-1}), respectively, V is the volume of the adsorption solution (L), and m is the mass of MB (g).

The Langmuir and Freundlich isotherm models are represented by the Eq. (3) [23,24]:

$$\text{Langmuir model: } q_e = \frac{q_m k_L C_e}{1 + K_L C_e} \tag{3}$$

where q_e is the equilibrium adsorption amount of MB in the aqueous solution by the ECD-GO/Fe_3O_4 composite (mg g^{-1}), q_m is the maximum equilibrium adsorption amount of MB in the aqueous solution by the ECD-GO/Fe_3O_4 composite (mg g^{-1}), C_e is the residual concentration of MB after equilibrium adsorption under different conditions (mg L^{-1}), and k_L is the Langmuir model binding constant (L mg^{-1}).

$$\text{Freundlich model: } q_e = k_F C_e^{1/n} \tag{4}$$

where q_e is the equilibrium adsorption amount of MB in the aqueous solution by the ECD-GO/Fe_3O_4 composite (mg g^{-1}), C_e is the residual concentration of MB after adsorption equilibrium under different conditions (mg L^{-1}), k_F is the Freundlich model adsorption equilibrium constant (mg L^{-1}), and n is the Freundlich model constant, indicating the inhomogeneity constant.

The pseudo-first-order and pseudo-second-order kinetic models are given by the Eq. (5) [25,26]:

$$\text{Pseudo-first-order kinetic model: } q_t = q_e\left(1 - e^{-k_1 t}\right) \tag{5}$$

where q_e is the equilibrium adsorption amount of MB in the aqueous solution by the geopolymer (mg g^{-1}), q_t is the equilibrium adsorption amount of MB in the aqueous solution by the ECD-GO/Fe_3O_4 at different time intervals (mg g^{-1}), t is the adsorption time (min), and k_1 is the pseudo-first-order kinetic model constant (min^{-1}).

Pseudo-second-order kinetic model: $q_t = \frac{k_2 q_e^2 t}{1 + k_2 q_e t}$ (6)

where q_e is the equilibrium adsorption amount of MB in the aqueous solution by the geopolymer (mg g^{-1}), q_t is the equilibrium adsorption amount of MB in the aqueous solution by the ECD-GO/Fe_3O_4 at different time intervals (mg g^{-1}), t is the adsorption time (min), and k_2 is the pseudo-second-order kinetic model constant (g mg^{-1} min^{-1}).

2.3. ECD-GO/Fe_3O_4 composite preparation

150 mg of GO and 300 mL of deionized water were added to a three-neck flask and sonicated for 2 h. Subsequently, 200 mg of KOH and 1.0 g of ECD were added. The mixture was then placed in an oil bath at 80°C. Ammonia (approximately 650 μL) and hydrazine hydrate (approximately 150 μL) were supplied continuously dropwise, and stirring was continued for 72 h. The precipitate obtained was ECD-GO. Centrifugal washing was then carried out with absolute ethanol to achieve neutrality. The mixture was then dried to obtain pure ECD-GO [27].

0.1 g of the prepared ECD-GO powder, 0.5 g $FeCl_3 \cdot 6H_2O$, 1.0 g of PEG, and 50 mL ethylene glycol were added to a beaker. The mixture was stirred for 2 h. Thereafter, 3.6 g of anhydrous NaAc and 1.0 g of PEG were added. The solution was then sealed in a 100 mL Teflon-lined autoclave and transferred into a 200°C drying oven for 16 h. After cooling to room temperature, centrifugal washing with H_2O and absolute ethanol was performed to achieve neutrality. The mixture was then dried to obtain ECD-GO/Fe_3O_4. The product preparation process is illustrated in Fig. 1.

3. Structure characterization

3.1. Fourier transform infrared spectroscopy (FT-IR) analysis

The KBr tablet method was used to obtain the infrared spectra (the mass ratio of the sample to KBr was 1:80). The results are shown in Fig. 2.

As can be seen in Fig. 2a, 3,438 and 1,635 cm^{-1} corresponded to the vibrational absorption and stretching vibration peaks of –OH and C=O, respectively. It can be judged that these groups are functional groups in GO. 1,386 cm^{-1} corresponded to the stretching vibration peak of C–OH, and 1,077 and 1,152 cm^{-1} corresponded to the stretching vibration peaks of C–O. Compared with (a), curve (b) showed new peaks at 2,922 and 2,360 cm^{-1}, attributable to the stretching vibration peaks of –CH_2–. The peak at 1,027 cm^{-1} corresponded to the stretching vibration peak of C–N on ethylenediamine. In addition, the peak at 3,310 cm^{-1} is consistent with the tensile vibration peak of –NH– and –OH at 3,438 cm^{-1}, and the intensity is significantly enhanced, which proves that ECD has been loaded onto the GO surface. Go forms strong hydrogen bonds with ECD groups. During the adsorption process, ECD-GO has a synergistic promotion effect on MB adsorption due to electrostatic interaction with cationic dyes in water, van der Waals force hydrogen bond interaction and stereoscopic effect. In Fig. 2c, the lattice absorption peak of Fe–O appeared at 602 cm^{-1}, indicating the formation of the ECD-GO/Fe_3O_4 complex.

3.2. Thermogravimetric analysis (TGA)

The TGA curves of ECD-GO/Fe_3O_4 were obtained by heating the composite to 700°C at the heating rate of 100°C/min in air. The results are shown in Fig. 3.

From Fig. 3, it can be seen that the weight loss of ECD-GO/Fe_3O_4 at 110°C or below was approximately 3.1% in the measured temperature range. The weight loss from

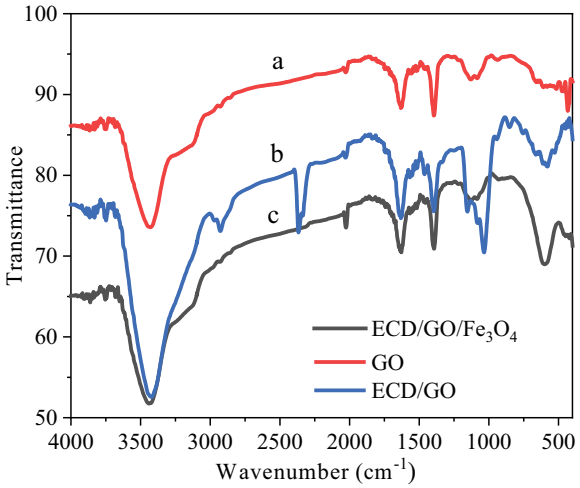

Fig. 2. FT-IR spectra of (a) GO, (b) ECD-GO, and (c) ECD-GO/Fe_3O_4.

Fig. 1. Illustration of the synthesis process of ECD-GO/Fe_3O_4.

110–260°C was approximately 29.1%, which was mainly because of the decomposition of ethylene diamine cyclodextrin. Compared with (a), from 260–500°C, the loss in mass was reduced by about 30.2%, corresponding to the corresponding to the mass proportion of Fe_3O_4. The preliminary conclusion that can be drawn is that the mass ratio of GO was approximately 28.4% in ECD-GO/Fe_3O_4. Thus, the mass ratios of ECD, GO, and Fe_3O_4 nanoparticles in the composite were approximately 29.1%, 28.4%, and 30.2%, respectively.

3.3. Transmission electron microscopy (TEM)

The electron acceleration voltage of TEM was 100 kV. The TEM results for the composite are shown in Fig. 4.

As shown in Fig. 4a, ECD was assembled on the surface of flaky graphene in the form of spheres, which confirmed the successful synthesis of the ECD-GO supramolecular system. In Fig. 4b it can be observed that the ECD-GO/Fe_3O_4 morphology did not change significantly. The grain size ranged from 60–70 nm.

3.4. Magnetic performance analysis

The magnetic properties of ECD-GO/Fe_3O_4 were analyzed through vibrating sample magnetometry (VSM) at room temperature. The results are demonstrated in Fig. 5.

As can be observed in Fig. 5, the coercivity of both Fe_3O_4 and ECD-GO/Fe_3O_4 nanoparticles was zero, proving that they have superparamagnetic properties. The saturation magnetization of Fe_3O_4 was 62 emu g^{-1} and that of ECD-GO/Fe_3O_4 was weakened to 22 emu g^{-1} due to its interaction with the non-magnetic material ECD-GO.

4. Adsorption properties of the composite toward MB

4.1. Adsorption isotherms

To study the adsorption mechanism of MB on the complex, adsorption experiments were carried out at room temperature with different initial MB concentrations (20, 40, 60, 80, 100, and 120 mg/L). The relationship between the equilibrium adsorption amount and the equilibrium concentration can be obtained by adopting the Langmuir and Freundlich models. The adsorption isotherm curves of MB are illustrated in Fig. 6 (t = 30 min, pH = 7).

As can be seen from Fig. 6, the adsorbent removal rate of MB increased with the additional amounts and then tended to attain equilibrium. The saturated adsorption capacity was approximately 53 mg/g. From the curves in the figure,

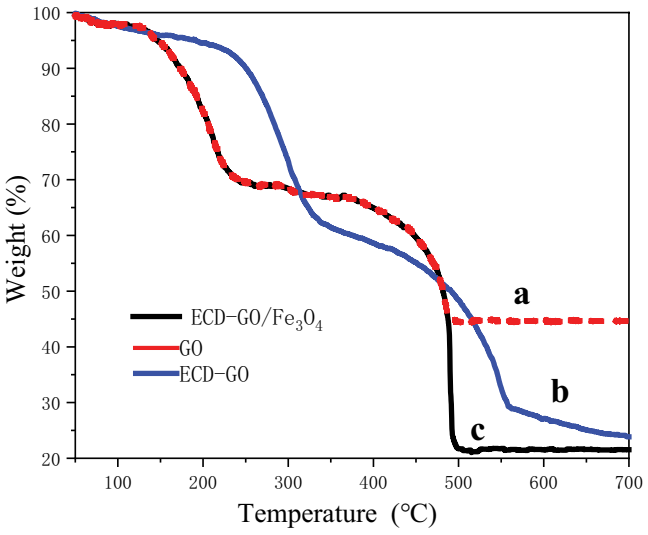

Fig. 3. TGA curves of (a) GO, (b) ECD-GO, and (c) E-CD-GO/Fe_3O_4.

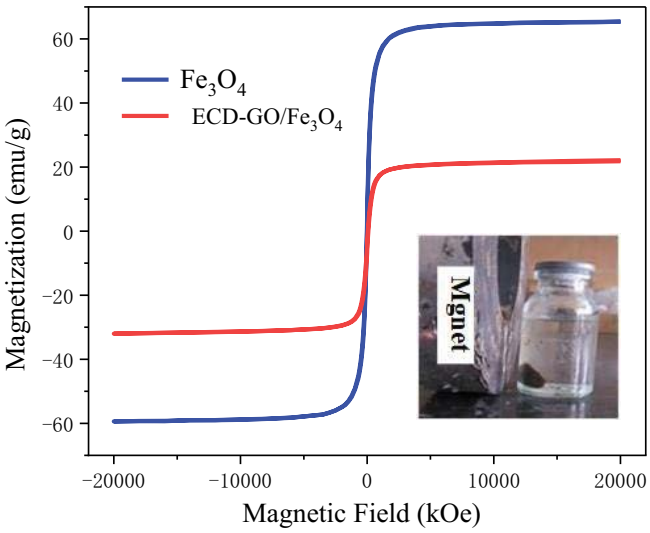

Fig. 5. Magnetization curves of nano-Fe_3O_4 and ECD-GO/Fe_3O_4.

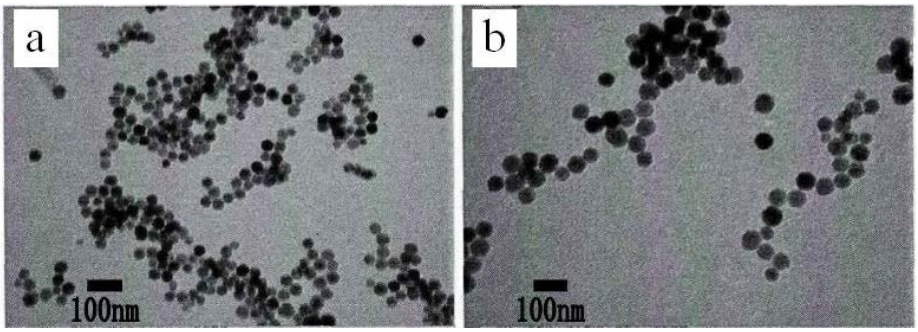

Fig. 4. TEM images of (a) ECD-GO and (b) ECD-GO/Fe_3O_4.

the decorrelation coefficient of the Langmuir model was R^2 = 0.85 and that of the Freundlich model was R^2 = 0.96. The adsorption isotherm process was more in line with the Freundlich equation and K_L was positive, indicating that the adsorption process was spontaneous at room temperature until the available exchangeable sites reached their limits [28,29].

4.2. Adsorption kinetics

To analyze the adsorption rate of MB by the complex, its static kinetics curves (Fig. 7) were obtained from the batch experiments and analyzed using the pseudo-first-order and pseudo-second-order equations.

As can be seen from Fig. 7, at the initial adsorption stage, the surface of the composite exposed more active sites, so the adsorption capacity increased rapidly. Further, the initial concentration of MB in the solution was high, which was favorable for adsorption. With the increase in time, the rising trend gradually slowed down, and the adsorption capacity did not change significantly. This could be because the surface of the complex was covered by the adsorbed MB and the concentration gradient of MB between the surface of the adsorbent and the solution was small, which was unfavorable for adsorption. This trend of fast-to-slow adsorption behavior has been extensively reported in the literature [21,26,30]. Firstly, the experimental data were used to dynamically fit the composite material, and then the adsorption kinetics curve and kinetic parameters of mb on the composite material were determined. According to Fig. 7, the correlation coefficients of pseudo-first-order and pseudo-second-order models are R^2 = 0.94 and R^2 = 0.91, respectively. Therefore, the adsorption kinetic process is more consistent with the pseudo-first-order equation.

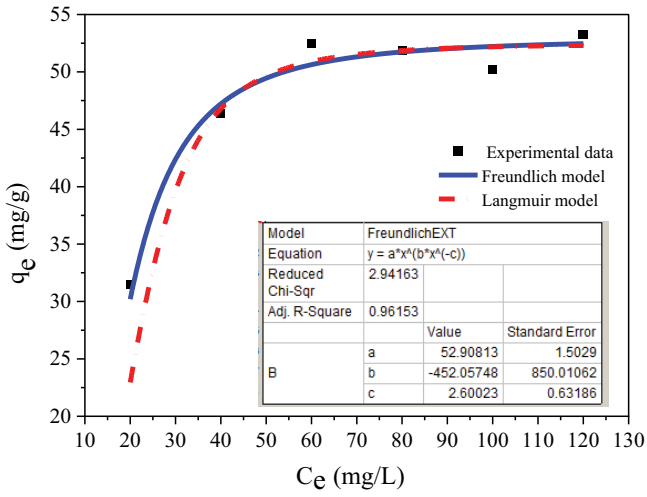

Fig. 6. Adsorption isotherms curves of MB on the composite (t = 30min, pH = 7).

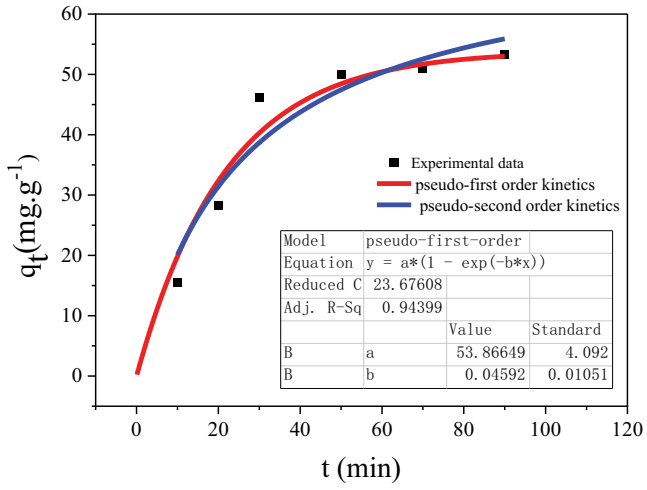

Fig. 7. Effect of adsorption time on MB removal by the composite.

4.3. Effect of pH on adsorption performance

The effect of solution pH on MB adsorption performance is shown in Fig. 8, where it can be seen that the change in pH value caused an evident change in MB removal. When the pH of the solution was 8, its adsorption effect was the best. MB is a cationic dye, and the hydroxyl, amino, and carboxyl groups on GO and ECD are protonated, resulting in electrostatic repulsion with the MB cations under acidic conditions. In addition, high concentrations of H^+ compete with MB ions for the adsorption sites [31], which is not conducive to adsorption. When the pH was greater than 8, the adsorption capacity was reduced due to the influence of van der Waals forces and π–π bonding interactions during the adsorption process [32].

4.4. Recycling study

The reproducibility of the ECD-GO/Fe_3O_4 complex is one of the important indicators for evaluating its adsorption performance. The complex was recovered, soaked in 1 mol/L HCl solution for 5 h after adsorption, washed with deionized water several times to remove residual HCl, dried in vacuum, and then used for adsorption. The results are illustrated in Fig. 9.

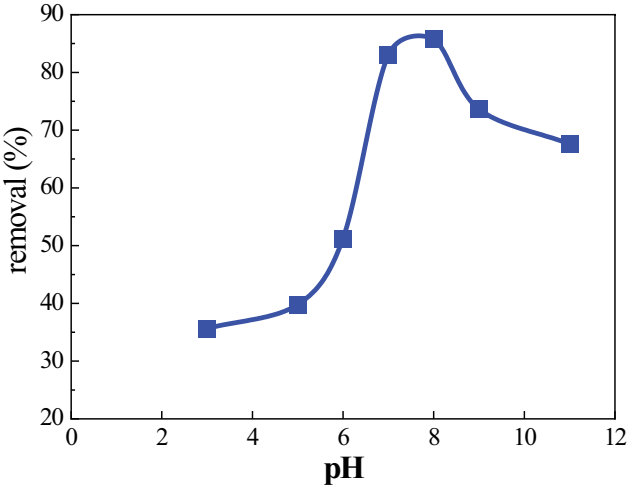

Fig. 8. Effect of pH on MB removal.

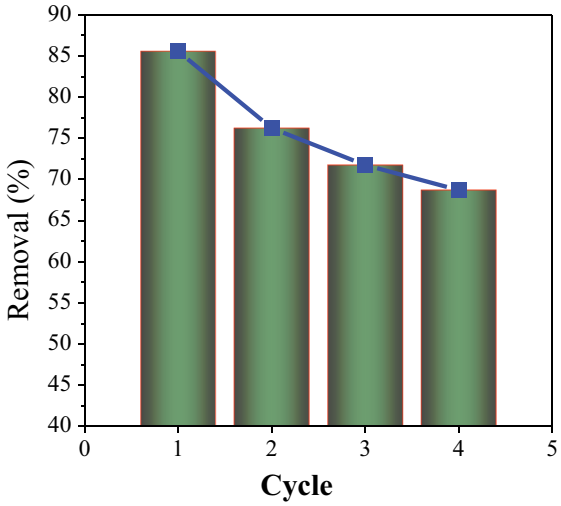

Fig. 9. Cyclic utilization of ECD-GO/Fe_3O_4 for MB removal.

It can be seen from Fig. 9 that the removal rate remained at about 69% after four cycles, indicating that ECD-GO/Fe_3O_4 has high stability and durability.

5. Conclusion

In this study, ECD-GO supramolecules were synthesized from ECD and GO, and Fe_3O_4 nanoparticles were loaded to obtain magnetic nanocomposite ECD-GO/Fe_3O_4. Among the three synthetic materials, cyclodextrin and graphene gradually decompose at a high temperature of 500°C, indicating that the materials have high stability and durability. In addition, the mass percentages of the raw materials were determined, and the mass ratios of ECD, GO and nano Fe_3O_4 were about 29.1%, 28.4% and 30.2%, respectively. This shows that the three raw materials have uniform quality and are ternary composite adsorbents. According to the microstructure characterization and magnetic property analysis, the Fe_3O_4 particles show a spherical diameter of 60–70 nm, which makes the composite maintain the superparamagnetic properties of 22 egu g^{-1}. ECD-GO/Fe_3O_4 can remove 87.9% of MB at pH 8 through electrostatic interaction and hydrogen bonding with cationic dyes, and the adsorption process occurs spontaneously at room temperature, which proves that the synthesized nanocomposites can effectively treat MB-containing wastewater. Through the above analysis and characterization, this experiment fully demonstrated for the first time the successful loading of Fe_3O_4 with simple operation process and low energy consumption on ECD-GO, which made the adsorbent achieve better separation effect. Therefore, the green, environmental and recyclable properties of graphene and its derivatives are comprehensively realized.

Acknowledgments

The financial support for this research by the National Natural Science Foundation of China (21968035, U2003123) and the Provincial Natural Science Foundation of Xinjiang Uygur Autonomous Region (2020D01C021) are gratefully acknowledged.

References

[1] S. Velusamy, A. Roy, S. Sundaram, T.K. Mallick, A review on heavy metal ions and containing dyes removal through graphene oxide-based adsorption strategies for textile wastewater treatment, The Chemical Rec.; J. Chem. Soc. Jpn., 21 (2021) 1570–1610.
[2] F. Saleem Ahmed Khan, N. Mujawar Mubarak, Y. Hua Tan, M. Khalid, R. Rao Karri, R. Walvekar, E. Chan Abdullah, S. Nizamuddin, S. Ali Mazari, A comprehensive review on magnetic carbon nanotubes and carbon nanotube-based buckypaper for removal of heavy metals and dyes, J. Hazard. Mater., 413 (2021) 125375, doi: 10.1016/j.jhazmat.2021.125375.
[3] R. Kishor, D. Purchase, G. Dattatraya Saratale, R.G. Saratale, L.F. Romanholo Ferreira, M. Bilal, R. Chandra, R. Naresh Bharagava, Ecotoxicological and health concerns of persistent coloring pollutants of textile industry wastewater and treatment approaches for environmental safety, J. Environ. Chem. Eng., 9 (2021) 105012, doi: 10.1016/j.jece.2020.105012.
[4] A. Saravanan, P. Senthil Kumar, S. Jeevanantham, S. Karishma, B. Tajsabreen, P.R. Yaashikaa, B. Reshma, Effective water/wastewater treatment methodologies for toxic pollutants removal: processes and applications towards sustainable development, Chemosphere, 280 (2021) 130595, doi: 10.1016/j.chemosphere.2021.130595.
[5] T.A. Kurniawan, Z. Mengting, D. Fu, S.K. Yeap, M.H. Dzarfan Othman, R. Avtar, T. Ouyang, Functionalizing TiO2 with graphene oxide for enhancing photocatalytic degradation of methylene blue (MB) in contaminated wastewater, J. Environ. Manage., 270 (2020) 110871, doi: 10.1016/j.jenvman.2020.110871.
[6] C. Zhao, W. Chen, A review for tannery wastewater treatment: some thoughts under stricter discharge requirements, Environ. Sci. Pollut. Res., 26 (2019) 26102–26111.
[7] K. Piaskowski, R. Świderska-Dąbrowska, P.K. Zarzycki, Dye removal from water and wastewater using various physical, chemical, and biological processes, J. AOAC Int., 101 (2018) 1371–1384.
[8] D. Vishnu, B. Dhandapani, S. Authilingam, S.V. Sivakumar, A comprehensive review of effective adsorbents used for the removal of dyes from wastewater, Curr. Anal. Chem., 18 (2022) 255–268.
[9] P. Samanta, A.V. Desai, S. Let, S.K. Ghosh, Advanced porous materials for sensing, capture and detoxification of organic pollutants toward water remediation, ACS Sustainable Chem. Eng., 7 (2019) 7456–7478.
[10] P.T.L. Huong, N. Tu, H. Lan, N. Van Quy, P.A. Tuan, N.X. Dinh, V.N. Phan, A.-T. Le, Functional manganese ferrite/graphene oxide nanocomposites: effects of graphene oxide on the adsorption mechanisms of organic MB dye and inorganic As(V) ions from aqueous solution, RSC Adv., 8 (2018) 12376–12389.
[11] S.Z.N. Ahmad, W.N.W. Salleh, A.F. Ismail, N. Yusof, M.Z.M. Yusop, F. Aziz, Adsorptive removal of heavy metal ions using graphene-based nanomaterials: toxicity, roles of functional groups and mechanisms, Chemosphere, 248 (2020) 126008, doi: 10.1016/j.chemosphere.2020.126008.
[12] H. Zeng, W. Qi, L. Zhai, F. Wang, J. Zhang, D. Li, Preparation and characterization of sludge-based magnetic biochar by pyrolysis for methylene blue removal, Nanomaterials, 11 (2021) 2473, doi: 10.3390/nano11102473.
[13] P.L. Yap, M.J. Nine, K. Hassan, T.T. Tung, D.N.H. Tran, D. Losic, Graphene-based sorbents for multipollutants removal in water: a review of recent progress, Adv. Funct. Mater., 31 (2021) 2007356, doi: 10.1002/adfm.202007356.
[14] M.F. Hossain, N. Akther, Y. Zhou, Recent advancements in graphene adsorbents for wastewater treatment: current status and challenges, Chin. Chem. Lett., 31 (2020) 2525–2538.
[15] J.R. Lead, G.E. Batley, P.J.J. Alvarez, M.-N. Croteau, R.D. Handy, M.J. McLaughlin, J.D. Judy, K. Schirmer, Nanomaterials in the environment: behavior, fate, bioavailability, and effects—an updated review, Environ. Toxicol. Chem., 37 (2018) 2029–2063.
[16] S. Wang, H. Sun, H.M. Ang, M.O. Tadé, Adsorptive remediation of environmental pollutants using novel graphene-based nanomaterials, Chem. Eng. J., 226 (2013) 336–347.

[17] K.C. Kemp, H. Seema, M. Saleh, N.H. Le, K. Mahesh, V. Chandra, K.S. Kim, Environmental applications using graphene composites: water remediation and gas adsorption, Nanoscale, 5 (2013) 3149–3171.
[18] C. Muankaew, P. Saokham, P. Jansook, T. Loftsson, Self-assembly of cyclodextrin complexes: detection, obstacles and benefits, Die Pharmazie, 75 (2020) 307–312.
[19] Z. Yang, X. Liu, X. Liu, J. Wu, X. Zhu, Z. Bai, Preparation of β-cyclodextrin/graphene oxide and its adsorption properties for methylene blue, Colloids Surf., B, 200 (2021) 111605, doi: 10.1016/j.colsurfb.2021.111605.
[20] R.K.S. Rathour, J. Bhattacharya, A. Mukherjee, β-Cyclodextrin conjugated graphene oxide: a regenerative adsorbent for cadmium and methylene blue, J. Mol. Liq., 282 (2019) 606–616.
[21] L.-W. Jiang, F.-T. Zeng, Y. Zhang, M.-Y. Xu, Z.-W. Xie, H.-Y. Wang, Y.-X. Wu, F.-A. He, H.-L. Jiang, Preparation of a novel Fe_3O_4/graphite oxide nanosheet/citric acid-crosslinked β-cyclodextrin polymer composite to remove methylene blue from water, Adv. Powder Technol., 32 (2021) 492–503.
[22] T. Ahamad, Mu. Naushad, G.E. Eldesoky, S.I. Al-Saeedi, A. Nafady, N.S. Al-Kadhi, A.H. Al-Muhtaseb, A.A. Khan, A. Khan, Effective and fast adsorptive removal of toxic cationic dye (MB) from aqueous medium using amino-functionalized magnetic multiwall carbon nanotubes, J. Mol. Liq., 282 (2019) 154–161.
[23] M.U. Tahir, X. Su, M. Zhao, Y. Liao, R. Wu, D. Chen, Preparation of hydroxypropyl-cyclodextrin-graphene/Fe_3O_4 and its adsorption properties for heavy metals, Surf. Interfaces, 16 (2019) 43–49.
[24] T. Ahamad, Mu. Naushad, G.E. Eldesoky, S.I. Al-Saeedi, A. Nafady, N.S. Al-Kadhi, A.H. Al-Muhtaseb, A.A. Khan, A. Khan, Effective and fast adsorptive removal of toxic cationic dye (MB) from aqueous medium using amino-functionalized magnetic multiwall carbon nanotubes, J. Mol. Liq., 282 (2019) 154–161.
[25] F.A. Ugbe, N. Abdus-Salam, Kinetics and thermodynamic modelling of natural and synthetic goethite for dyes scavenging from aqueous systems, Arabian J. Sci. Eng., 7 (2020) 12–28.
[26] B.T. Gemici, H.U. Ozel, H.B. Ozel, Removal of methylene blue onto forest wastes: adsorption isotherms, kinetics and thermodynamic analysis, Environ. Technol. Innovation, 22 (2021) 101501, doi: 10.1016/j.eti.2021.101501.
[27] J. Liu, G. Chen, M. Jiang, Supramolecular hybrid hydrogels from noncovalently functionalized graphene with block copolymers, Macromolecules, 44 (2011) 7682–7691.
[28] M. Bounaas, A. Bouguettoucha, D. Chebli, J.M. Gatica, H. Vidal, Role of the wild carob as biosorbent and as precursor of a new high-surface-area activated carbon for the adsorption of methylene blue, Arabian J. Sci. Eng., 46 (2021) 325–341.
[29] Y. Kuang, X. Zhang, S. Zhou, Adsorption of methylene blue in water onto activated carbon by surfactant modification, Water, 12 (2020) 587, doi: 10.3390/w12020587.
[30] L. Mouni, L. Belkhiri, J.-C. Bollinger, A. Bouzaza, A. Assadi, A. Tirri, F. Dahmoune, K. Madani, H. Remini, Removal of methylene blue from aqueous solutions by adsorption on kaolin: kinetic and equilibrium studies, Appl. Clay Sci., 153 (2018) 38–45.
[31] Mu. Naushad, A.A. Alqadami, Z.A. AlOthman, I.H. Alsohaimi, M.S. Algamdi, A.M. Aldawsari, Adsorption kinetics, isotherm and reusability studies for the removal of cationic dye from aqueous medium using arginine modified activated carbon, J. Mol. Liq., 293 (2019) 111442, doi: 10.1016/j.molliq.2019.111442.
[32] Y. Ai, Y. Liu, Y. Huo, C. Zhao, L. Sun, B. Han, X. Cao, X. Wang, Insights into the adsorption mechanism and dynamic behavior of tetracycline antibiotics on reduced graphene oxide (RGO) and graphene oxide (GO) materials, Environ. Sci.: Nano, 6 (2019) 3336–3348.